MultiCraft

International Journal of Engineering, Science and Technology
Vol. 8, No. 2, 2016, pp. 1-10

INTERNATIONAL JOURNAL OF ENGINEERING, SCIENCE AND TECHNOLOGY

www.ijest-ng.com
www.ajol.info/index.php/ijest

Unsteady MHD flow in porous media past over exponentially accelerated inclined plate with variable wall temperature and mass transfer along with Hall current

Uday Singh Rajput and Gaurav Kumar*

Department of Mathematics, Lucknow University, Lucknow(226007), U.P, India.
**Corresponding Author: e-mail: rajputgauravlko@gmail.com, Tel +918574005045.*

Abstract

In this paper we are studying unsteady MHD flow in porous media past over exponentially accelerated inclined plate having variable wall temperature as well as mass transfer along with Hall current. We have used Laplace-transform technique to find the solution of the equations in the flow model. The results obtained are discussed with the help of graphs. The drag force at the boundary has been tabulated.

Keywords: MHD, unsteady flow, inclined plate, Hall current, skin friction.

DOI: http://dx.doi.org/10.4314/ijest.v8i2.1

1. Introduction

The MHD flow plays important roles in different areas of science and technology, like chemical engineering, mechanical engineering, petroleum engineering, biomechanics, irrigation engineering and aerospace technology. A number of researchers have worked on MHD flow considering the different flow models. In most of the models heat and mass are the prime components. Some of the models are worth mentioning. Hall effect on MHD flow through a speed up plate was investigated in Deka (2008). Seth et al. (2010) have analyzed convective flow of the unsteady MHD type in a rotating channel surrounded by parallel plate having thermal source/sink in a porous medium in slip boundary states. Rajput and Sahu (2011) have investigated effects of rotation and magnetic field on the flow past an exponentially accelerated vertical plate with constant temperature.

Chauhan and Rastogi (2012) have analyzed Hall effect on MHD slip-flow as well as heat transfer by a porous mode above a speed up plate within a revolving system. Mukherjee and Prasad (2014) have analyzed influence of radiation as well as porosity factor on MHD flow as a result of exponentially-stretching sheet for a porous channel. Srinivas and Kishan (2015) have considered Hall effects on unsteady MHD free convection flow over a stretching sheet with variable viscosity and viscous dissipation. We are considering the unsteady MHD flow over an exponentially-accelerated inclined plate having heat as well as mass transfer through porous medium with Hall current's occurrence. The results are disused with the help of graphs and table.

2. Mathematical analysis

Geometric model of the problem is shown in Figure 1.

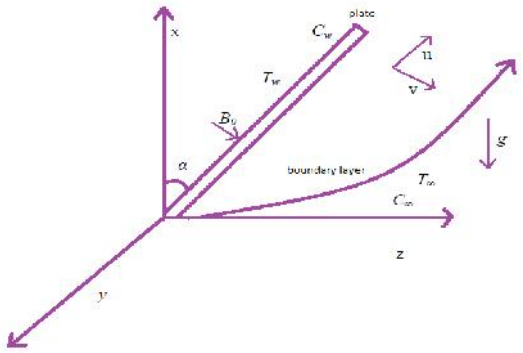

Figure 1. Geometric model of the problem

The x axis is along the vertical which is normal to y-z plane. The z axis lies in the horizontal plane. The plate is inclined at angle α from vertical. A uniform magnetic field $B=(0,0,B_0)$ is employed perpendicular to the flow. During the motion, the direction of the magnetic field changes along with the plate in such a way that it always remains perpendicular to it. This means, the direction of magnetic field is tied with the plate. Let (u, v, w) be the components of the velocity vector V. Then using the equation of continuity $\nabla.V=0$, we get w=0.

The equation of generalized ohm's law is given as

$$j+\frac{\mu_e^2 e}{B_0}(j\times B)=\pm(E+V\times B).$$

However the external electric field due to polarization of charges is as negligible, therefore ***E=0***.

Thus the equation becomes

$$j+\frac{\mu_e^2 e}{B_0}(j\times B)=\pm(V\times B).$$

Here $m(=\mu_e^2 e)$ is the Hall current parameter. ω_e and τ_e are the cyclotron frequency and the collision time of electrons, respectively. Other symbols are as usual. Let (j_1, j_2, j_3) be the components of current density ***j***. Here J_1 is the current density along the flow, and J_2 is perpendicular to it. Since J_3 component is along the plate which is non-conducting, therefore J_3 =0.

Using above assumption, generalized ohm's law gives $j_1+mj_2=\pm vB_0$ and $j_2-mj_1=-\pm uB_0$.

Solving these equations, we get $j_1=\frac{\pm B_0(v+mu)}{1+m^2}$ and $j_2=\frac{\pm B_0(mv-u)}{1+m^2}$.

Further, flow through porous media is governed by the following form of Darcy's Law $q=\frac{-K}{\mu}\nabla \boldsymbol{p},$ where q is the flux (discharge per unit area with unit length per unit time), ∇p is pressure gradient while K is the medium's intrinsic permeability. The relation between Darcy's flux and porosity is given by $V=\frac{q}{\phi},$ where V is fluid velocity and ϕ is the porosity of the medium.

These equations are combined with Navier-Stokes equation to obtain the flow model under study.

Equations of motion

$$\frac{\partial u}{\partial t}=\nu\frac{\partial^2 u}{\partial z^2}+g\ Cos\sim(T-T_\infty)+g\ ^*Cos\sim(C-C_\infty)-\frac{\pm B_0^2(u+mv)}{\rho(1+m^2)}-\frac{\nu u}{K}, \quad (1)$$

$$\frac{\partial v}{\partial t}=\nu\frac{\partial^2 v}{\partial z^2}+\frac{\pm B_0^2(mu-v)}{\rho(1+m^2)}-\frac{\nu v}{K}, \quad (2)$$

Diffusion equation

$$\frac{\partial C}{\partial t}=D\frac{\partial^2 C}{\partial z^2}, \quad (3)$$

Equation of energy

$$\circ C_p \frac{\partial T}{\partial t} = k \frac{\partial^2 T}{\partial z^2}. \tag{4}$$

The conditions at the boundary of the flow could be stated as:

$$\left.\begin{aligned} &t \le 0 : u = 0,\ v = 0,\ T = T_\infty,\ C = C_\infty,\ \forall z, \\ &t > 0 : u = u_0 e^{bt},\ v = 0,\ T = T_\infty + (T_w - T_\infty)\frac{u_0^2 t}{\upsilon},\ C = C_\infty + (C_w - C_\infty)\frac{u_0^2 t}{\upsilon},\ \text{at } z=0, \\ &u \to 0,\ v \to 0,\ T \to T_\infty,\ C \to C_\infty \ \text{as } z \to \infty. \end{aligned}\right\} \tag{5}$$

Here, *u* is the primary velocity, v- secondary velocity, *g*- gravitational acceleration, β-volumetric coeff. of thermal expansion, *b*-acceleration parameter, *t*- time, *m*- the Hall current, *K*-the permeability parameter, *T*-temp of the fluid, β^*-volumetric coeff. of concentration expansion, *C*-concentration of the fluid, ¬ -the kinematic viscosity, ρ- density, C_p- specific heat, *k*-thermal conductivity of the fluid, *D*- mass diffusion coeff., T_w-temperature near the plate, C_w-species concentration near the plate, B_0-magnetic parameter.

Now to transform equations (1), (2), (3) and (4) into dimensionless form, the following dimensionless quantities are introduced

$$\left.\begin{aligned} &\bar{z} = \frac{z u_0}{\nu}, \bar{u} = \frac{u}{u_0}, \bar{v} = \frac{v}{u_0}, \bar{} = \frac{(T - T_\infty)}{(T_w - T_\infty)}, S_c = \frac{\nu}{D}, \alpha = \circ \nu, P_r = \frac{\alpha c_p}{k}, G_r = \frac{g \beta (T_w - T_\infty)}{u_0^3}, \\ &M = \frac{\pm B_0^2 \nu}{\circ u_0^2}, G_m = \frac{g \beta^* (C_w - C_\infty)}{u_0^3}, \bar{b} = \frac{b \nu}{u_0^2}, \bar{C} = \frac{(C - C_\infty)}{(C_w - C_\infty)}, \bar{t} = \frac{t u_0^2}{\nu}, \bar{K} = \frac{u_0}{\nu^2} K. \end{aligned}\right\} \tag{6}$$

Here $\bar{u}$ is dimensionless primary velocity, $\bar{v}$ – secondary velocity, $\bar{b}$ -dimensionless acceleration parameter, $\bar{t}$ – dimensionless time, $\bar{}$ – dimensionless temperature, $\bar{C}$ – dimensionless concentration, $\bar{K}$ – the dimensionless permeability parameter, G_r – the thermal Grashof number, G_m – the mass Grashof number, α – coeff. of viscosity, P_r – Prandtl number, S_c – Schmidt number, *M*-magnetic parameter.

Thus the model becomes

$$\frac{\partial \bar{u}}{\partial \bar{t}} = \frac{\partial^2 \bar{u}}{\partial \bar{z}^2} + G_r Cos\sim \bar{} + G_m Cos\sim \bar{C} - \frac{M(\bar{u} + m\bar{v})}{(1 + m^2)} - \frac{1}{\bar{K}}\bar{u}, \tag{7}$$

$$\frac{\partial \bar{v}}{\partial \bar{t}} = \frac{\partial^2 \bar{u}}{\partial \bar{z}^2} + \frac{M(m\bar{u} - \bar{v})}{(1 + m^2)} - \frac{1}{\bar{K}}\bar{v}, \tag{8}$$

$$\frac{\partial \bar{C}}{\partial \bar{t}} = \frac{1}{S_c}\frac{\partial^2 \bar{C}}{\partial \bar{z}^2}, \tag{9}$$

$$\frac{\partial \bar{}}{\partial \bar{t}} = \frac{1}{P_r}\frac{\partial^2 \bar{}}{\partial \bar{z}^2}. \tag{10}$$

The boundary conditions (5) become:

$$\left.\begin{aligned} &\bar{t} \le 0 : \bar{u} = 0, \bar{v} = 0, \bar{} = 0, \bar{C} = 0, \quad \forall\, \bar{z}, \\ &\bar{t} > 0 : \bar{u} = e^{\bar{b}\bar{t}}, \bar{v} = 0, \bar{} = \bar{t}, \bar{C} = \bar{t}, \quad \text{at } \bar{z} = 0, \\ &\bar{u} \to 0, \bar{v} \to 0, \bar{} \to 0, \bar{C} \to 0, \quad \text{as } \bar{z} \to \infty. \end{aligned}\right\} \tag{11}$$

For convenience, we remove the bars in the above equations to get

$$\frac{\partial u}{\partial t}=\frac{\partial^2 u}{\partial z^2}+G_r Cos\sim^{-}+G_m Cos\sim C-\frac{M(u+mv)}{(1+m^2)}-\frac{1}{K}u, \tag{12}$$

$$\frac{\partial v}{\partial t}=\frac{\partial^2 v}{\partial z^2}+\frac{M(mu-v)}{(1+m^2)}-\frac{1}{K}v, \tag{13}$$

$$\frac{\partial C}{\partial t}=\frac{1}{S_c}\frac{\partial^2 C}{\partial z^2}, \tag{14}$$

$$\frac{\partial^{-}}{\partial t}=\frac{1}{P_r}\frac{\partial^{2-}}{\partial z^2}. \tag{15}$$

The corresponding boundary conditions become:

$$\left.\begin{array}{l} t\le 0: u=0, v=0, ^{-}=0, C=0, \quad \forall z, \\ t>0: u=e^{bt}, v=0, ^{-}=t, C=t \quad \text{at z=0,} \\ \mathrm{u}\to 0,\ \mathrm{v}\to 0,\ \theta\to 0,\ \mathrm{C}\to 0, \quad \text{as } z\to\infty. \end{array}\right\} \tag{16}$$

Combining equations (12) and (13), the model becomes

$$\frac{\partial q}{\partial t}=\frac{\partial^2 q}{\partial z^2}+G_r Cos\sim^{-}+G_m Cos\sim C-qa, \tag{17}$$

$$\frac{\partial C}{\partial t}=\frac{1}{S_c}\frac{\partial^2 C}{\partial z^2}, \tag{18}$$

$$\frac{\partial^{-}}{\partial t}=\frac{1}{P_r}\frac{\partial^{2-}}{\partial z^2}. \tag{19}$$

Finally, the boundary conditions become:

$$\left.\begin{array}{l} t\le 0: q=0, ^{-}=0, C=0, \quad \forall z, \\ t>0: q=e^{bt}, ^{-}=t, C=t, \quad \text{at z=0,} \\ q\to 0, ^{-}\to 0, C\to 0, \quad \text{as } z\to\infty. \end{array}\right\} \tag{20}$$

Here $q = u + i\,v$, $a = \dfrac{M\,(1 - im)}{1 + m^2} + \dfrac{1}{K}$.

The equations (17) to (19), are solved by Laplace - transform method. The solution obtained is as under:

$$q=\frac{1}{2}e^{bt-\sqrt{a+bz}}A_{15}+\frac{Cos\sim}{4a^2\sqrt{\circledR}}[\sqrt{\circledR}G_r\{-A_9 z+\sqrt{a}e^{-\sqrt{a}z}A_2 z+\frac{1}{2A_{13}A_3}+2e^{-\sqrt{a}z}A_1P_r+2A_{13}A_3P_r\}-G_rP_r\{-aA_{10}z+$$

$$\frac{1}{\sqrt{P_r}}A_{13}\sqrt{\circledR}A_4+\frac{2\sqrt{\circledR}A_{11}}{\sqrt{P_r}}-\frac{2a\sqrt{\circledR}tA_{11}}{\sqrt{P_r}}+\frac{1}{A_{13}\sqrt{\circledR}A_8\sqrt{P_r}}-2\sqrt{\circledR P_r}A_{11}\}-\sqrt{\circledR}G_m\{A_9 z-\sqrt{a}e^{-\sqrt{a}z}A_2 z-2e^{-\sqrt{a}z}A_1S_c+$$

$$2A_{14}A_5S_c\}+\sqrt{S_c}G_m\{-aA_{16}z+\frac{1}{\sqrt{\circledR S_c}A_{14}A_7}+\frac{2\sqrt{\circledR}A_{12}}{\sqrt{S_c}}+\frac{1}{A_{14}\sqrt{\circledR S_c}A_6}-2A_{12}\sqrt{\circledR S_c}\}].$$

$$C = t\left\{(1+\frac{z^2 S_c}{2t})erfc[\frac{\sqrt{S_c}}{2\sqrt{t}}] - \frac{z\sqrt{S_c}}{\sqrt{\circledR\sqrt{t}}} e^{-\frac{z^2}{4t}} S_c\right\},$$

$$- = t\left\{(1+\frac{z^2 P_r}{2t})erfc[\frac{\sqrt{P_r}}{2\sqrt{t}}] - \frac{z\sqrt{P_r}}{\sqrt{\circledR\sqrt{t}}} e^{-\frac{z^2}{4t}} P_r\right\},$$

The expressions for the symbols involved in the solution are mentioned in the appendix.

3. Skin Friction

The non-dimensional skin-friction is given as

$$\left(\frac{dq}{dz}\right)_{z=0} = {}^{2}x + i^{2}y \cdot$$

4. Analysis of the results

The velocity profiles for various parameters like thermal and mass Grashof numbers, magnetic parameter (M), Hall current (m), acceleration parameter (b), permeability parameter (K), Prandtl number (Pr) and time (t) are shown in Figures 1.1 to 2.10. It is deduced from Figures 1.1 and 2.1 that primary and secondary velocities of fluid decrease when the angle of inclination (α) is increased. It is observed from Figure 1.2 and 2.2, when the mass Grashof number Gm is increased then the velocities are increased. From Figures 1.3 and 2.3 it is deduced that velocities increase with Gr. Further we observe that when permeability parameter K is increased then the velocities are increased (Figures 1.4 and 2.4), which is obvious due to the fact that increase in porosity helps in free movement of the fluid particles. Hence it is in agreement with the natural flow of the fluid. Also, if Hall current parameter m is increased then u increases, while v gets decreased (Figures 1.5 and 2.5). It is observed from Figures 1.6 and 2.6 that when M increases, u decreases, but the trend reverses with v. Further, we see that when acceleration parameter b is increased then the velocities are increased (Figures 1.7 and 2.7). This is again in agreement with the natural flow of the fluid. From Figures 1.8, 2.8, 1.9 and 2.9, it can be seen that the velocities u and v decrease when Pr and Sc are increased. Further, from Figures 1.10 and 2.10, it is observed that velocities increase with time. This is due to the fact that plate is accelerated continuously. Finally we state that the theoretical results are in agreement with the natural flow phenomenon.

Skin friction is given in Table 1. The value of τ_x rises with the rise in Gm, Gr, m, K and t. However, it decreases with α, M, b, Pr and Sc. Similar effects are observed with τ_y, except M, b and m. Further, when M and b are increased then τ_y increases. Again, τ_y decreases when m increases. Comparative plots of τ_x and τ_y for Hall current and magnetic field parameter are shown in Figures 3.1 and 3.2, respectively.

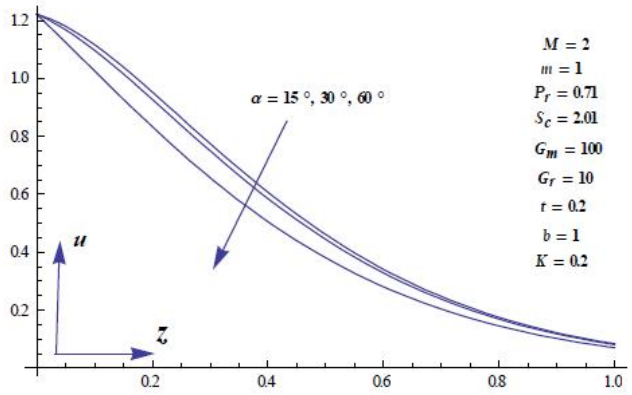

Figure1.1: u vs z

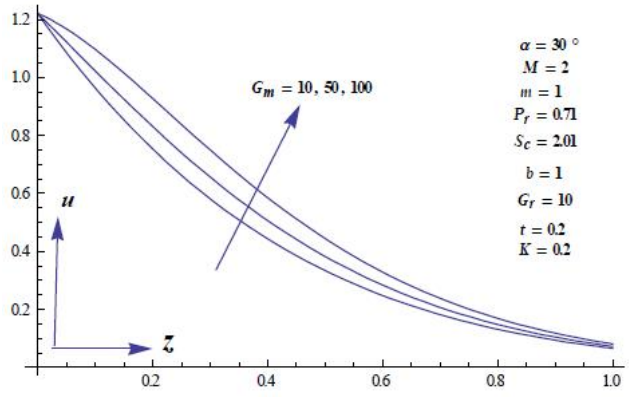

Figure1.2: u vs z

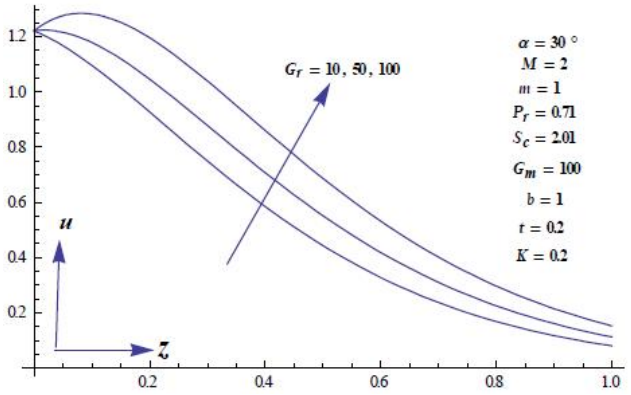

Figure1.3: *u vs z*

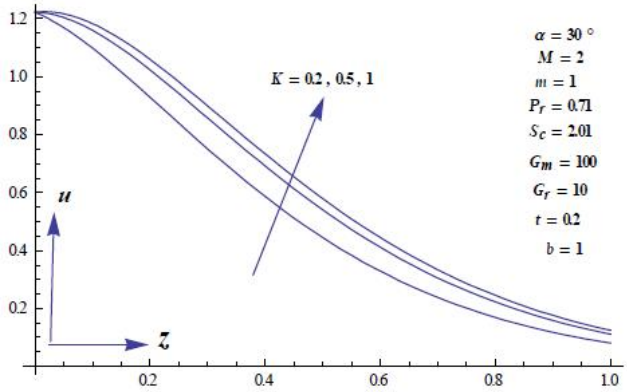

Figure1.4: *u vs z*

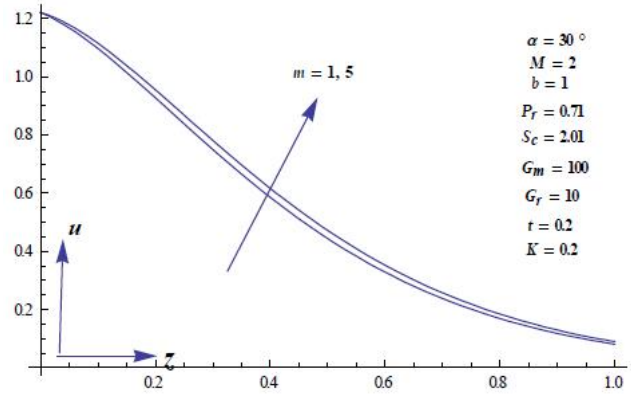

Figure1.5: *u vs z*

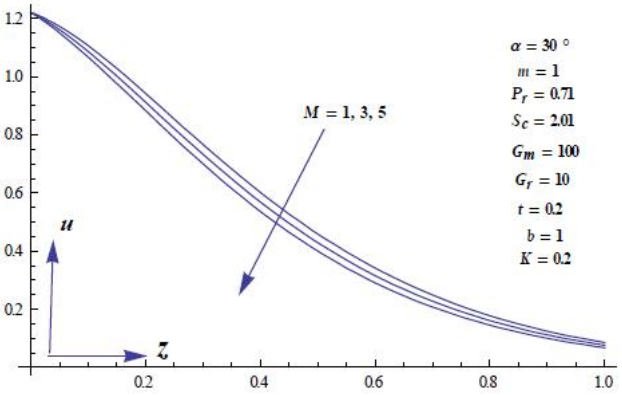

Figure1.6: *u vs z*

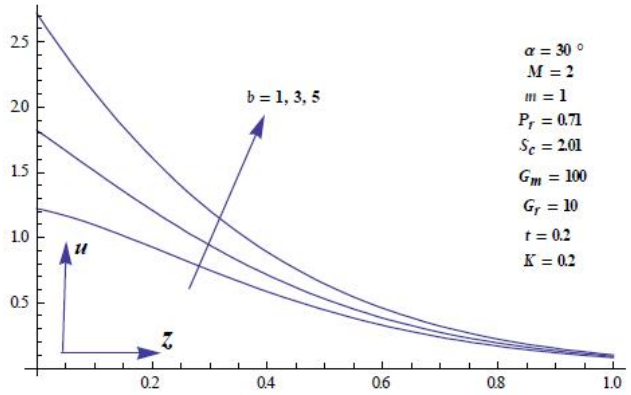

Figure1.7: *u vs z*

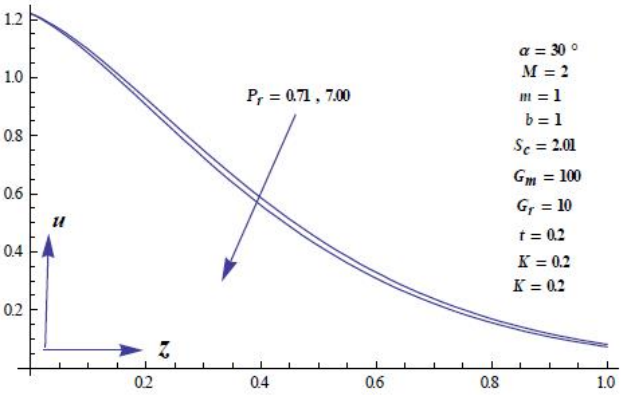

Figure1.8: *u vs z*

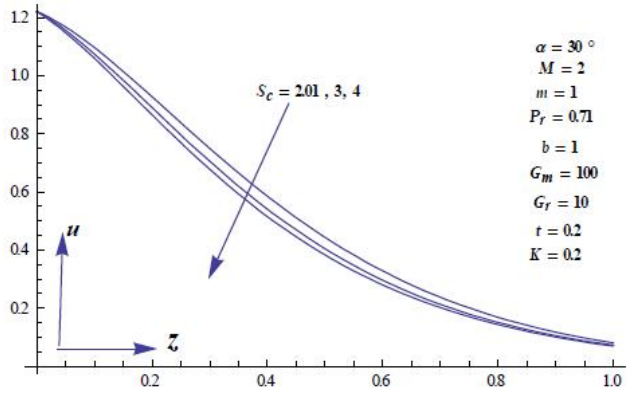

Figure1.9: *u vs z*

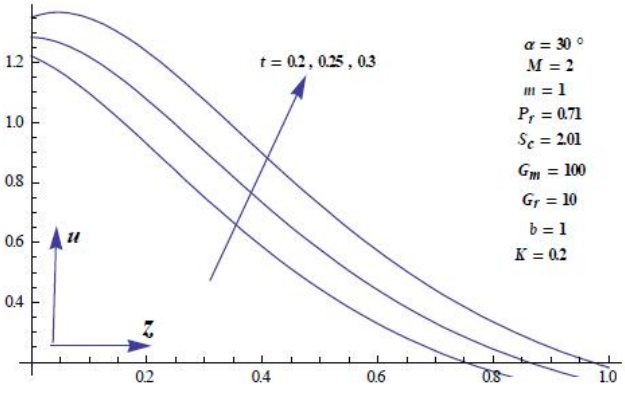

Figure1.10: *u vs z*

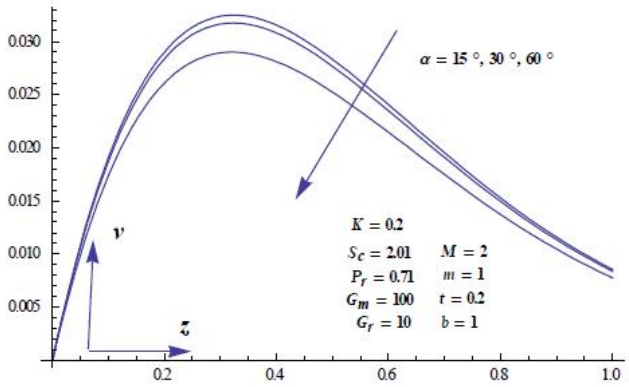

Figure2.1: *v vs z*

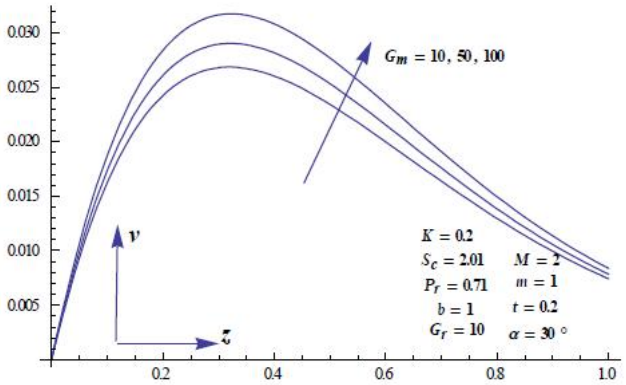

Figure2.2: *v vs z*

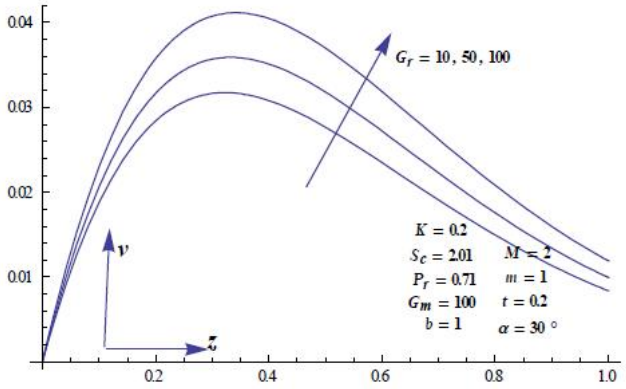

Figure2.3: *v vs z*

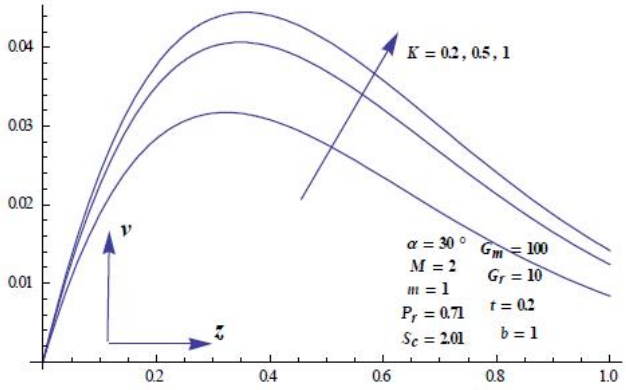

Figure2.4: *v vs z*

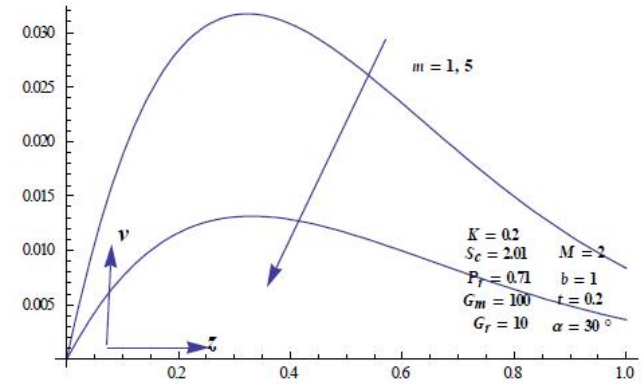

Figure2.5: *v vs z*

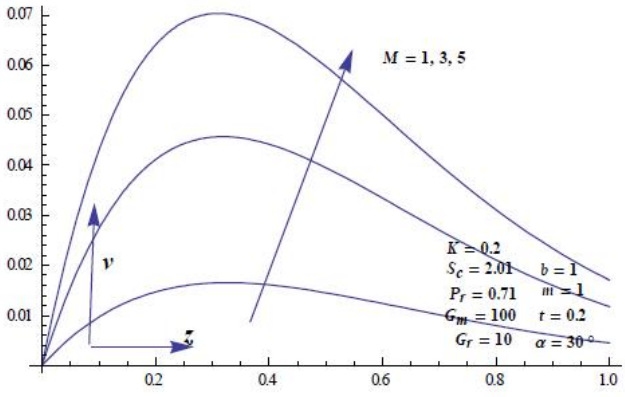

Figure2.6: *v vs z*

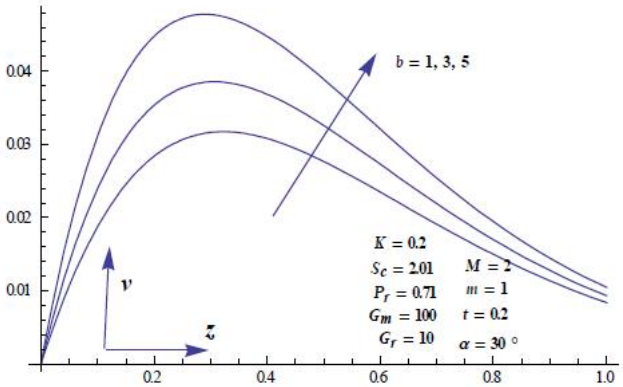

Figure2.7: *v vs z*

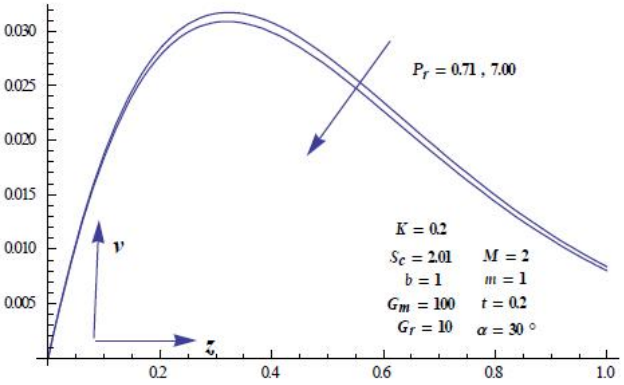

Figure2.8: *v vs z*

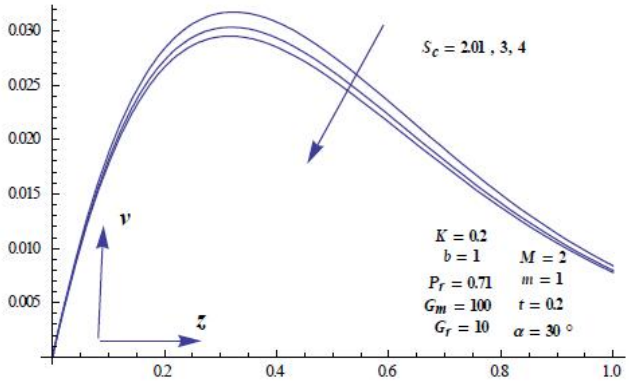

Figure2.9: v vs z

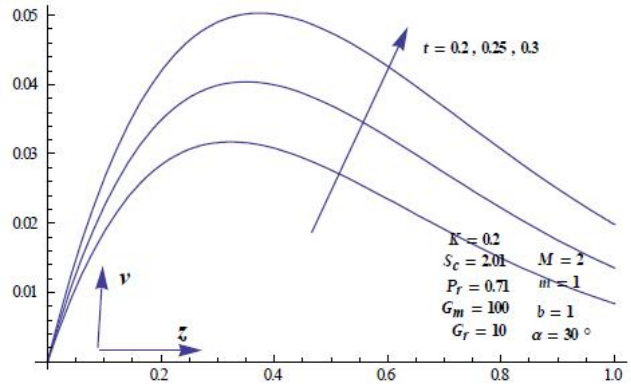

Figure2.10: v vs z

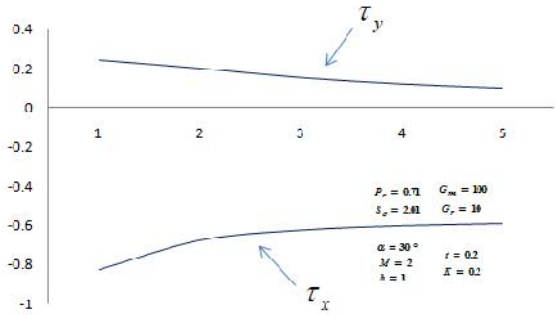

Figure 3.1: τ_x and τ_y vs m

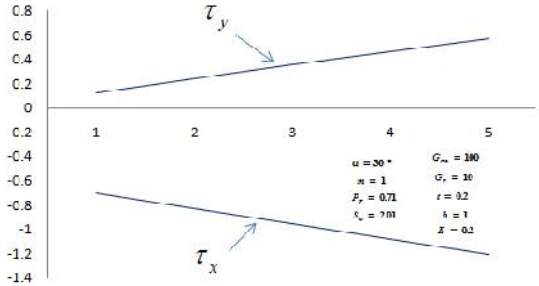

Figure 3.2: τ_x and τ_y vs M

Table 1. Skin friction for different parameters

α (in degree)	M	m	Pr	Sc	Gm	Gr	b	K	t	τ_x	τ_y
15	2	1	0.71	2.01	100	10	1	0.2	0.2	-0.541468	0.247678
30	2	1	0.71	2.01	100	10	1	0.2	0.2	-0.827971	0.243668
60	2	1	0.71	2.01	100	10	1	0.2	0.2	-1.877690	0.228976
30	1	1	0.71	2.01	100	10	1	0.2	0.2	-0.700557	0.124738
30	3	1	0.71	2.01	100	10	1	0.2	0.2	-0.954858	0.357087
30	4	1	0.71	2.01	100	10	1	0.2	0.2	-1.081000	0.465289
30	5	1	0.71	2.01	100	10	1	0.2	0.2	-1.206222	0.568562
30	2	2	0.71	2.01	100	10	1	0.2	0.2	-0.604172	0.119536
30	2	3	0.71	2.01	100	10	1	0.2	0.2	-0.625872	0.151797
30	2	4	0.71	2.01	100	10	1	0.2	0.2	-0.604172	0.119536
30	2	5	0.71	2.01	100	10	1	0.2	0.2	-0.593376	0.097892
30	2	1	7.00	2.01	100	10	1	0.2	0.2	-0.958664	0.240115
30	2	1	0.71	3.00	100	10	1	0.2	0.2	-1.061420	0.237563
30	2	1	0.71	4.00	100	10	1	0.2	0.2	-1.224650	0.233724
30	2	1	0.71	2.01	10	10	1	0.2	0.2	-2.810190	0.216816
30	2	1	0.71	2.01	50	10	1	0.2	0.2	-1.929210	0.228750
30	2	1	0.71	2.01	100	50	1	0.2	0.2	0.2967940	0.263373
30	2	1	0.71	2.01	100	100	1	0.2	0.2	1.7027500	0.288004
30	2	1	0.71	2.01	100	10	2	0.2	0.2	-1.810370	0.278891
30	2	1	0.71	2.01	100	10	3	0.2	0.2	-3.052660	0.327170
30	2	1	0.71	2.01	100	10	4	0.2	0.2	-4.620360	0.320717

Table 1. (cont'd): Skin friction for different parameters

α (in degree)	M	m	Pr	Sc	Gm	Gr	b	K	t	τ_x	τ_y
30	2	1	0.71	2.01	100	10	5	0.2	0.2	-6.595070	0.429615
30	2	1	0.71	2.01	100	10	1	0.5	0.2	-0.0432093	0.282300
30	2	1	0.71	2.01	100	10	1	1.0	0.2	0.2462720	0.298052
30	2	1	0.71	2.01	100	10	1	0.2	0.3	0.7779030	0.328436
30	2	1	0.71	2.01	100	10	1	0.2	0.4	2.5355800	0.428897

5. Conclusion

The flow model considered in the research has been solved by Laplace transform technique. The model consists of equations of motion, diffusion equation and equation of energy. To study the solutions obtained, standard sets of the values of the parameters have been considered. The numerical data obtained is discussed with the help of graphs and table. We found that the data obtained is in concurrence with the actual flow phenomenon.

Appendix

$$A_1 = -1 - A_{16} - e^{2\sqrt{a}z}(1 - A_{17}),\ A_2 = -1 + A_{16} - e^{2\sqrt{a}z}(1 - A_{17}),\ A_8 = -A_4,\ A_3 = -1 + A_{20} - A_{18}(1 - A_{21}),$$

$$A_4 = 1 + A_{23} + A_{18}(1 - A_{24}),\ A_5 = -1 + A_{25} - A_{19}(1 - A_{26}),\ A_6 = -1 - A_{27} - A_{19}(1 + A_{28}),\ A_7 = -A_6,\quad A_9 = \frac{2e^{-\sqrt{a}z}A_1}{z}(1 - at),$$

$$A_{10} = (2e^{\frac{-z^2P_r}{4t}}\sqrt{t} + \sqrt{®}\,zA_{11})\sqrt{P_r},\ A_{11} = -1 + erf\,[\frac{z\sqrt{P_r}}{2\sqrt{t}}],\ A_{12} = -1 + erf\,[\frac{z\sqrt{S_c}}{2\sqrt{t}}],\ A_{13} = e^{\frac{at}{-1+P_r} - z\sqrt{\frac{aP_r}{-1+P_r}}}$$

$$,\ A_{14} = e^{\frac{at}{-1+S_c} - z\sqrt{\frac{aS_c}{-1+S_c}}},\ A_{15} = 1 + A_{29} + e^{2\sqrt{a+b}z}A_{30},\ A_{16} = erf\,[\frac{2\sqrt{a}t - z}{2\sqrt{t}}],\ A_{17} = erf\,[\frac{2\sqrt{a}t + z}{2\sqrt{t}}]$$

$$,\ A_{18} = e^{-2z\sqrt{\frac{aP_r}{-1+P_r}}},\ A_{19} = e^{-2z\sqrt{\frac{aS_c}{-1+S_c}}}\cdot\ A_{20} = erf\,[\frac{z - 2t\sqrt{\frac{aP_r}{-1+P_r}}}{2t}],\ A_{21} = erf\,[\frac{z + 2t\sqrt{\frac{aP_r}{-1+P_r}}}{2t}],$$

$$A_{22} = erf\,[\frac{2t\sqrt{\frac{a}{-1+P_r}} - z\sqrt{P_r}}{2t}],\ A_{23} = erf\,[\frac{2t\sqrt{\frac{a}{-1+P_r}} - z\sqrt{P_r}}{2t}],\ A_{24} = erf\,[\frac{2t\sqrt{\frac{a}{-1+P_r}} + z\sqrt{P_r}}{2t}],\ A_{25} = erf\,[\frac{z - 2t\sqrt{\frac{aS_c}{-1+S_c}}}{2t}],$$

$$A_{26} = erf\,[\frac{z + 2t\sqrt{\frac{aS_c}{-1+S_c}}}{2t}],\ A_{27} = erf\,[\frac{2t\sqrt{\frac{a}{-1+S_c}} - 2\sqrt{S_c}}{2t}],\ A_{28} = erf\,[\frac{2t\sqrt{\frac{a}{-1+S_c}} + 2\sqrt{S_c}}{2t}],$$

$$A_{29} = erf\,[\frac{2\sqrt{a+b}t - z}{2\sqrt{t}}],\ A_{30} = erfc\,[\frac{2\sqrt{a+b}t + z}{2\sqrt{t}}],$$

References

Chauhan .D. S. and Rastogi. P., 2012. Hall effects on MHD slip flow and heat transfer through a porous medium over an accelerated plate in a rotating system, *International Journal of Nonlinear Science*, Vol. 14, No. 2, pp.228-236

Deka R.K., 2008. Hall effects on MHD flow past an accelerated plate, *Theoretical and Applied Mechanics*, Vol. 35, No.4, pp. 333-346.

Mukherjee B. and Prasad N., 2014. Effect of radiation and porosity parameter on hydromagnetic flow due to exponentially stretching sheet in a porous media, *International Journal of Engineering, Science and Technology*, Vol. 6, No. 1, pp. 58-70.

Rajput U. S. and Sahu. P. K., 2011. Effects of rotation and magnetic field on the flow past an exponentially accelerated vertical plate with constant temperature, International Journal of Mathematical Archive, Vol. 2, No. 12, pp 2831-2843

Seth G.S., Nandkeolyar R. and Ansari M. S. 2010. Unsteady MHD convective flow within a parallel plate rotating channel with thermal source/sink in a porous medium under slip boundary conditions, *International Journal of Engineering, Science and Technology*, Vol. 2, No. 11, 2010, pp. 1-16

Srinivas M and Kishan N, 2015. Hall effects on unsteady MHD free convection flow over a stretching sheet with variable viscosity and viscous dissipation, *World Applied Sciences Journal*, Vol. 33, No. 6, pp. 1032-1041.

Biographical notes

Dr Uday Singh Rajput is a permanent faculty member in the department of mathematics and astronomy, Lucknow University, India. He has more than 25 years of teaching experience at UG and PG levels and also guided students for PhD degree. He has published more than 60 research articles. His research areas include MHD flows, Graph Theory and Operations Research.
.

Gaurav Kumar is research student in the department of mathematics and astronomy, Lucknow University, India.

Received April 2016
Accepted May 2016
Final acceptance in revised form May 2016